Faster entanglement production driven by quantum resonance in many-body rotors

Sanku Paul,[1] J. Bharathi Kannan,[2] and M.S. Santhanam[2]

[1] *Department of Physics and Complex Systems, S.N. Bose National Centre for Basic Sciences, Kolkata 700106, India*
[2] *Department of Physics, Indian Institute of Science Education and Research, Pune 411008, India*

Quantum resonance in the paradigmatic kicked rotor model is a purely quantum effect that ignores the state of underlying classical chaos. In this work, the effect of quantum resonance on entanglement generation in the N-interacting kicked rotors is studied. We show a compelling feature: entanglement growth is superlinear in time until the timescale t^*, beyond which the entanglement production slows down to a logarithmic profile with superimposed oscillations. Notably, we find that at resonance, the entanglement dynamics is independent of the kick strength of rotors, but depends solely on the interaction strength. By mapping positional interaction to momentum space and analytically calculating the linear entropy, we elucidate the underlying mechanism driving these distinct growth profiles. The analytical findings are in excellent agreement with the numerical simulations performed for two- and three-interacting kicked rotors. Our results are amenable to an experimental realization on ultracold atom setup.

Quantum entanglement captures the degree of non-local correlation between two groups of particles and serves as a crucial resource for quantum technologies, *e.g.*, quantum computation [1], teleportation [2, 3], and secure communication [4]. In many-body quantum systems, entanglement as quantified by the von-Neumann entropy $S_{\rm vN}$ carries signatures of the quantum phases and the phase transitions [5]. For instance, in ergodic phase, $S_{\rm vN}$ grows linearly with time before saturating. In non-ergodic many-body localized phases, asymptotically, $S_{\rm vN}$ displays an even slower logarithmic growth with time. As entanglement is a useful resource for quantum technologies, faster than linear rate of generating entanglement, *e.g.*, superlinear growth rate, will be useful in many practical settings.

In recent years, efforts has been made to generate faster entanglement. Interestingly, it has been achieved in non-Hermitian PT-symmetric systems in the vicinity of exceptional points at which the eigenlevels and eigenstates coalease. Exceptional points can appear when two externally driven non-Hermitian qubits are weakly coupled together. Then, in parameteric regime close to an exceptional point, entanglement between the qubits is generated over a timescale much faster than the inverse of coupling strength [6, 7]. Another variant of fast entanglement generation problem appeals to quantum speed limit in the framework of Mandelstamm and Tamm [8–10] for achieving (maximally) entangled states such as GHZ and Werner states, starting from product states, using optimised Hamiltonians that can saturate the quantum speed limit bounds [11]. In the former case, enhanced entanglement rate depends on being in the vicinity of an exceptional point, which itself will require a system that is capable of displaying an exceptional point. In the latter case, a target entangled state is necessary to verify if quantum speed limit lower bound is saturated or not. In both these cases, rate of entanglement generation is not an asymptotic effect and also depends on factors such as the choice of initial states and symmetry of the system.

In contrast to these studies [6, 11], we study entanglement growth rates in interacting many-body chaotic quantum systems. Early results using two-body chaotic models such as kicked tops have shown that, for short times, entanglement growth is linear with a rate proportional to classical Lyapunov exponent [12]. In interacting systems, presence of many-body localized effects slows down entanglement growth, asymptotically, to logarithmic increase with time. Then, it is natural to ask if faster-than-linear entanglement production is possible. In this work, we provide an affirmative answer and that too has been obtained in a Hermitian time-dependent many-body quantum system with a chaotic classical limit.

Hence, in this work, we consider N-interacting quantum kicked rotors (QKR) set to be at resonance. The off-resonant QKR and its variants are one of the extensively studied paradigms in chaotic dynamics, both theoretically [13–16] and through experiments [17, 18]. It serves as a rich platform for exploring various phenomena such as quantum-classical correspondence [18–20], decoherence [21, 22], quantum ratchet [23, 24], and several others. The off-resonant QKR is characterized by the emergence of dynamical localization indicating a suppression of energy growth with time [25]. In contrast, resonant QKR ignores the underlying classical dynamics, and the quantum energy growth is ballistic: $\langle E\rangle \sim t^2$ [26]. The resonance and off-resonance conditions of QKR are distinguished by their driving frequency, a feature exploited in experiments for frequency discrimination [27]. Furthermore, QKR at resonance has been used to study topological phases [28, 29] and has also found application in atom interferometers [30]. Resonant conditions on interacting QKR systems have been studied yet.

The two-body quantum kicked rotor (TB-QKR) is a well-studied instance of a general coupled N-body QKR. The former displays dynamical phases ranging from localization [31] to diffusion [32]. The entanglement dynamics of TB-QKR defined with cylindrical boundary conditions (momentum space is unbounded but the position space has a periodic boundary condition) displays initial linear growth akin to the ergodic many-body system and is followed by a logarithmic growth [32]. In contrast, the TB-QKR with toral boundary conditions (both momentum and position have periodic boundary condition) displays initial linear growth followed by a saturation arising from finite size of Hilbert space [33–35]. However, it has been shown in ref. [36] that depending on the coherence of the initial state and for small interaction strengths, a super-linear entanglement growth is observed at short times followed by a linear growth and ultimately leads to saturation. Importantly, all these studies are focused particularly on the off-resonance condition of QKR. A natural question is how does this picture change at an on-resonance setting in many-body kicked rotors?

The main contribution of this work is towards unraveling the entanglement dynamics in N-interacting QKR, when the quantum resonance condition is satisfied. It is also worth highlighting that this is the first-ever study of entanglement dynamics in an N-interacting rotors. In this work, we show that the entanglement initially grows super-linearly succeeded by a logarithmic growth with a superimposed oscillation. We further show that the crossover time from super-linear to logarithmic growth depends inversely on the interaction strength. We obtain insight into the underlying mechanism driving the distinct entanglement growth profiles by analytically calculating a relatively simpler quantity, the linear entropy. Furthermore, we show that under a coordinate transformation, the N-interacting rotor problem at resonance reduces to a single-kicked rotor problem. Our analytical prediction is in excellent agreement with the numerical simulations. Additionally, we assert that entanglement not only limited to detecting phase transition in quantum many-body systems, but can also serve as a versatile probe capable of identifying resonance phenomena in N-interacting kicked rotors and thus detecting critical driving frequency in an experimental settings.

System: The Hamiltonian of the N-interacting kicked rotors is

$$H = \sum_{i=1}^{N} \frac{\tau_i p_i^2}{2} + [V_{\rm kick} + V_{\rm int}] \sum_n \delta(t - nT) \qquad (1)$$

where x_i and p_i are the position and momentum of the ith rotor with mass $1/\tau_i$. Here, we consider $\tau_i \in \mathbb{Z}$ and $\tau_i/\tau_j \neq 1$. The kicking potential is $V_{\rm kick} = \sum_{i=1}^{N} K_i \ \cos(x_i)$ with kick strength K_i. In this work, motivated by experiments, an all-to-all interaction between the rotors of the form $V_{\rm int} = K \ \cos\left(\sum_{i=1}^{N} x_i\right)$ is considered, where K is the interaction strength and T is the time period for the application of kick and interaction potentials: $V_{\rm kick}$ and $V_{\rm int}$. The interaction in the position space can be mapped to an interaction in the momentum space. In an experiment, interaction only in momentum space can be easily generated using two lasers with incommensurate frequencies [18]. To obtain the mapping, one needs to perform a coordinate transformation. For instance, consider two-interacting rotors with kick strength $K_i = 0, \ i = 1, 2$ in Eq. (1) and perform a coordinate transformation $\Theta = x_1 + x_2, \ \theta = x_1 - x_2, \ u = p_1 + p_2$, and $v = p_1 - p_2$. Under this transformation, the interaction in position gets mapped to the momentum space as ηuv, where $\eta = \tau_1 - \tau_2$. Consideration of $K_i = 0$ will become clear in the subsequent section. Several variants of two-interacting kicked rotors have been studied extensively [14, 32, 36, 37].

The quantum dynamics is obtained using the time-evolution operator $\mathcal{U} = (U_1 \otimes U_2 \otimes \cdots \otimes U_N) U_{\rm int}$, where

$$\begin{aligned} U_i &= U_i^{\rm free} U_i^{\rm kick} \\ &= \exp[-i\tau_i p_i^2 T/2\hbar_s] \exp[-iK_i \cos(x_i)/\hbar_s] \end{aligned} \qquad (2)$$

is the time-evolution operator of the i-th rotor and $\hbar_s$ is the scaled Planck's constant. The interaction appears as $U_{\rm int} = \exp[-iK \cos(\sum_{i=1}^{N} x_i)/\hbar_s]$. Now, starting with initial state chosen to be a product state, *i.e.* $|\psi(0)\rangle = |p_1 = 0\rangle \otimes |p_2 = 0\rangle \cdots |p_N = 0\rangle$, the time-evolved state is obtained as $|\psi(t)\rangle = \mathcal{U}|\psi(0)\rangle$. The resonance condition is incorporated by setting $\hbar_s T = 4\pi p/q$, where $p, q \in \mathbb{Z}$ [14]. In what follows, we fix $\hbar_s = 4\pi/T$ and $T = 12$. Due to this choice, $U_i^{\rm free}$ becomes an identity operation and does not contribute to the dynamics, and the resulting time-evolution operator is $\mathcal{U} = (U_1^{\rm kick} \otimes U_2^{\rm kick} \otimes \cdots \otimes U_N^{\rm kick}) U_{\rm int}$.

Entanglement is evaluated using the von-Neumann entropy $S_{\rm vN} = -{\rm Tr}_1 \rho_1 \ln \rho_1 = -\sum_j \lambda_j \ln \lambda_j$, where ρ_1 is the reduced density matrix of the rotor-1 obtained by tracing out the rest of the system and λ_j are the Schmidt eigenvalues of ρ_1. Figure 1(a) shows the growth of the entanglement for two-interacting kicked rotors. This shows two distinct growth profiles of entanglement. Contrary to the initial linear growth commonly observed in the chaotic regime, the entanglement (at resonance) grows super-linearly, as expressed by $S_{\rm vN} = t^{\mu}$ with $\mu = 1.6$; see left inset of Fig. 1(a). However, for $t > t^*$, entanglement grows logarithmically accompanied by an oscillation superimposed on it. Over time, the amplitude of this oscillation diminishes. Furthermore, the oscillation is a superposition of different frequencies. To the best of our knowledge, such distinct growth profiles have never been observed before. This result can be generalized to N-interacting kicked rotors, and entanglement for three rotors is shown in Fig. 3(b).

To gain more insight, we examine the Schmidt eigenvalues $\lambda_1 > \lambda_2 > \cdots > \lambda_N \geq 0$ of ρ_1. Figure 1(b) illustrates the behavior of $1 - \lambda_1$ over time, where λ_1 is the largest Schmidt eigenvalue that makes major contribution to $S_{\rm vN}$. It is evident from the Fig. 1(b) that $1 - \lambda_1$ initially exhibits a quadratic growth, which at later times $t > t^*$ displays logarithmic growth with an accompanying single-frequency oscillation. However, with time, the amplitude of oscillation vanishes. The initial

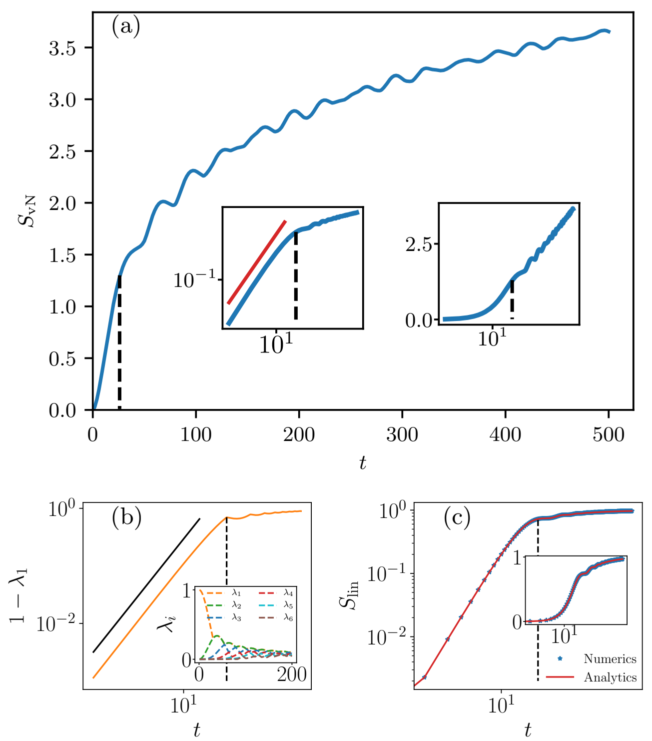

FIG. 1. (a) Time dynamics of the von-Neumann entropy of two-interacting kicked rotors is plotted. It displays two distinct growth profiles: (Left inset) Log-log plot illustrates the super-linear, $S_{\rm vN} \sim t^{1.6}$ growth of $S_{\rm vN}$ at initial times and (Right inset) Log-normal plot highlights the logarithmic growth with added oscillation at later times of $S_{\rm vN}$ growth. The black vertical dashed line in the main plot and the left inset represent the crossover time t^* between these two distinct growth profiles. The red solid line in the left inset is a fit to the super-linear growth. (b) Plot illustrates the quadratic growth of (1-λ_1), where λ_1 is the largest Schmidt eigenvalue of the reduced density matrix ρ_1, for $t < t^*$. The black solid line is the fit to this quadratic growth. Inset displays the time dynamics of the six largest Schmidt eigenvalues λ_i. (c) The linear entropy $S_{\rm lin}$ of two-interacting kicked rotors is plotted. Inset plots the log-normal of $S_{\rm lin}$ to highlight the oscillatory behavior of the late-time $S_{\rm lin}$ growth. The parameter sets are $K_1 = 4$, $K_2 = 5$, $K = 0.05$, $\tau_1 = 1$, $\tau_2 = 2$, $T = 12$, and basis size of each rotor, $L = 2^{10}$.

quadratic growth of $1 - \lambda_1$ can be understood following ref. [36, 37]. Despite being started with a zero momentum state, $|p_i = 0\rangle$ with $i = 1, 2$, as an initial state of both the rotors, the $|p_i = 0\rangle$ state can be expressed as a coherent superposition of the respective Floquet states $|p_i = 0\rangle = 1/\sqrt{L}\sum_{j=1}^{L} |\phi_j^i\rangle$, where $|\phi^i\rangle$ is the Floquet state of the ith rotor. Reference [36] explains that for such coherent states, λ_1 initially grows quadratically. The oscillation observed in $S_{\rm vN}$ being not of a single frequency can be understood from the inset of Fig. 1(b) which displays the largest six Schmidt eigenvalues. It can be noticed that each λ_i has its own distinct frequencies which gets nontrivially added up in the evaluation of $S_{\rm vN}$ resulting in such oscillation.

As a prelude to focussing on the oscillatory behavior, we emphasize that at resonance, as evident in Fig. 2(a), the kicking term in Eq. (1) does not contribute to the entanglement production. This implies that the entanglement growth with $K_i = 0$ is the same as that for $K_i \neq 0$. This leads us to a significant conclusion: Two distinct initial states of ith rotor yield the same entanglement dynamics. These are product states ; (a) $|\psi_i(0)\rangle = \sum_{n=1}^{L} J_n(K_i t/\hbar_s)|\phi_n^i\rangle = (U_i^{\rm kick})^t |p_i = 0\rangle$, when $K_i \neq 0$ and L is the basis size of each rotor, and (b) the zero momentum state $|p_i = 0\rangle$ for $K_i = 0$. While the initial state (a) is a coherent superposition of Floquet states, (b) is not so. Yet, these distinct type of states display super-linear entanglement growth followed by a logarithric growth with superimposed oscillations, a feature not observed before and could be useful in quantum resource theory [38].

For the reasons given above, we set $K_i = 0$ as it simplifies the analysis. Further, for reasons of analytical tractability, linear entropy is computed as entanglement indicator instead of the von Neumann entropy. The linear entropy is defined as $S_{\rm lin} = 1 - {\rm Tr}_A \rho_A^2$ and Fig. 1(c) displays its growth profile. It is evident from the inset of Fig. Fig. 1(c) that the linear entropy also exhibits oscillatory behavior at late times with a decreasing amplitude as time progresses. Evaluating $S_{\rm lin}$ crucially relies on determining the purity, expressed as $\mu_2 = {\rm Tr}_A \rho_A^2$. To do this, a coordinate transformation $\Theta = \sum_{i=1}^{N} x_i$ is performed that reduces the interaction term $U_{\rm int} = \exp[-iK\cos(\sum_{i=1}^{N} x_i)/\hbar_s]$ to that of effectively a "non-interacting" single particle kicking term $U_{\rm int} = \exp[-iK\cos(\Theta)/\hbar_s]$, while the interactions now appear as a complicated function $f(p_1, p_2, \ldots p_N, \tau_1, \tau_2, \cdots \tau_N)$ in the momentum space. At resonance, the free evolution term given by $U^{\rm free} = \exp[-if(p_1, p_2, \ldots p_N, \tau_1, \tau_2, \cdots \tau_N)T/2\hbar_s]$ becomes unity, and hence effectively reducing the many-body problem to that of a single-particle kicked rotor at resonance. In this context, the purity, $\mu_2 = \sum_j \lambda_i^2$, becomes equivalent to the participation ratio of a single kicked rotor ${\rm PR} = \sum_n |\psi_n|^4$. The Schmidt eigenvalues λ_i give the probability of finding the particle in Schmidt state $|\zeta_i\rangle$ of the ith rotor. For a single kicked rotor at resonance, it can be shown that ${\rm PR} = \sum_n J_n(Kt/\hbar_s)^4$, where $J_n(\cdot)$ is the Bessel function of first kind and order n. Thus, at resonance, the linear entropy of the N-interacting kicked rotors described in Eq. (1) is expressed as

$$S_{\rm lin} = 1 - \sum_n J_n(Kt/\hbar_s)^4 \,. \tag{3}$$

Figure 1(c) illustrates that the analytical result in Eq. (3) is in excellent agreement with the numerics. Furthermore, the analytical result for $S_{\rm lin}$ in Eq. Eq. (3) is not limited to two-interacting kicked rotors but remains valid for any number of interacting rotors described by

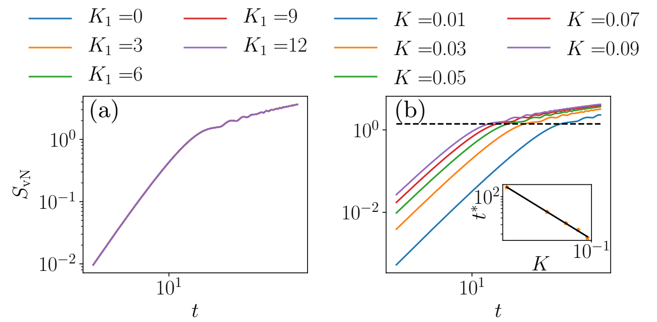

FIG. 2. The von-Neumann entropy $S_{\rm vN}$ of two-interacting kicked rotors is plotted for (a) different kicking strengths of rotor 1 (b) distinct interaction strength K. It illustrates the growth profile of $S_{\rm vN}$ is independent of K_1 while it strongly depends on K. Horizontal black dashed line in (b) corresponds to the critical $S^*_{\rm vN}$ after which the growth of $S_{\rm vN}$ changes its profile. It illustrates that $S^*_{\rm vN}$ is independent of K. Other parameters are same as in Fig. 1. The log-log plot in the inset of (b) signifies that the crossover time t^* inversely depends on coupling strength K following the relation $t^* \sim 1/K$.

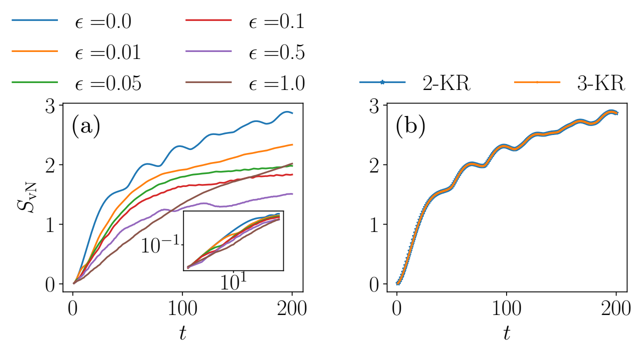

FIG. 3. (a) Plot demonstrates that the distinct growth profile of $S_{\rm vN}$ at resonance is highly sensitivity to the resonance condition. A slight deviation from the resonance condition significantly changes the growth profile of $S_{\rm vN}$. Inset displays the log-log plot of $S_{\rm vN}$ as a function of time. Color signifies the same values of ϵ as in the main plot. (b) Plot compares the growth profile of $S_{\rm vN}$ for two- and three-interacting kicked rotors. The kick strength of the third rotor is $K_3 = 5.5$ while the other parameters are the same as in Fig. 1.

the Hamiltonian in Eq. (1). This illustrates the generic nature of our findings.

How does the entanglement dynamics change with coupling strength K. Unlike the kicking strength K_i, the coupling strength K significantly influences the growth profile of $S_{\rm vN}$. This is evident in Fig. 2. With increasing K, numerical simulations in the inset of Fig. 2(b) shows that the crossover time t^* from super-linear to logarithmic growth decreases according to the relation $t^* \sim 1/K$. This reciprocal relation is in contrast to that observed at off-resonant single QKR where (linear) diffusive timescale follows $t^* \sim 1/K^2$ [32]. A plausible argument is that at resonance, the momentum distribution is not of a Gaussian profile, an essential condition required to observe the $1/K^2$ decay of t^*. Moreover, lacking of any analytical expression of the momentum distribution at resonance hinders the analytical calculation of t^*. Furthermore, the exponent μ of the super-linear growth $S_{\rm vN} \sim t^\mu$ is independent of the coupling strength as indicated in Fig. 2(b). Additionally, the critical entanglement value $S^*_{\rm vN}$ denoted by horizontal black dashed line in Fig. 2(b) after which $S_{\rm vN}$ changes its growth profile barely depends on the coupling strength K. Thus, the entanglement dynamics is strongly affected by interaction strength rather than the kick strength.

Dependence on $\hbar_s$: Next, we investigate how crucially the growth profile of entanglement observed in Fig. 1(a) depends on the resonance condition. To this end, the kick period T in Eq. (1) is varied through $T' = T + \epsilon$, where $\epsilon \ll T$, while maintaining the scaled Planck's constant as $\hbar_s = 4\pi/T$ thereby slightly deviating from resonance condition. Remarkably, Fig. 3(a) reveals that even a slight departure from the resonance condition markedly impacts the growth profile of entanglement. While the initial growth profile remains akin to that observed at resonance for small ϵ (see the inset in Fig. 3(a)), a significant deviation is noticed at later times. This is due to the fact that when $\epsilon > 0$, then the free evolution part $U_i^{\rm free}$ embedded in $\mathcal{U}$ begins to contribute. In turn, this results in the addition of phases that become significant as time progresses. Thus, even small ϵ leads the oscillation to vanish immediately. This is indicative of its sensitivity and holds considerable significance in experimental contexts. This further indicates the system's high-quality factor $Q = \frac{\nu_r}{\Delta\nu}$, where ν_r is the frequency of oscillation at resonance and $\Delta\nu$ denotes the half-width of the resonance curve. Thus, scanning through the lens of $\hbar_s$, we can precisely identify the resonance condition in an experiment.

Three-interacting kicked rotors: Here, we highlight the generic nature of the foregoing results. To demonstrate this, calculation of $S_{\rm vN}$ is extended to three-interacting kicked rotors. In particular, the entanglement of one rotor with the rest of the system is examined. Remarkably, the result displayed in Fig. 3(b) is identical to that observed for two-interacting rotors. This conclusively establishes the universality of our findings within the context of the interaction considered in Eq. (1). A remark is in order: For nearest-neighbor interaction of type $V_{\rm int} = \sum_i \cos(x_i - x_{i+1})$, the initial super-linear growth of $S_{\rm vN}$ is present, however, the amplitude of oscillation in the logarithmic regime dies out with the increase in number of rotors (not shown here).

In summary, the entanglement dynamics of all-to-all interacting kicked rotors under the resonance condition is studied. It reveals a novel paradigm: At initial times, the von-Neumann entropy displays super-linear growth. However, after a crossover time t^*, growth slows down to a logarithmic with oscillations superposed on it. The crossover time t^* depends inversely on the coupling strength between the rotors. It is further shown that for the all-to-all interaction considered in Eq. (1), *at resonance*, the kicking term, despite its role inducing chaos, does not contribute to the entanglement production. This effectively reduces the problem to that of a single-kicked rotor through a coordinate transformation. Given the challenges in analytically assessing von Neumann entropy, the evolution of a simpler quantity is examined, namely, linear entropy. This allows us to obtain analytical insights into the underlying mechanisms driving the observed growth profile of entanglement. These findings open a new frontier – faser than linear entanglement production not usually observed in chaotic systems. An immediate direction is to extend this investigation for other interaction potentials, namely, the point-to-point interaction and nearest-neighbor interaction.

[1] T. D. Ladd, F. Jelezko, R. Laflamme, Y. Nakamura, C. Monroe, and J. L. O'Brien, Nature **464**, 45–53 (2010).
[2] C. H. Bennett, G. Brassard, C. Crépeau, R. Jozsa, A. Peres, and W. K. Wootters, Phys. Rev. Lett. **70**, 1895 (1993).
[3] D. Bouwmeester, J.-W. Pan, K. Mattle, M. Eibl, H. Weinfurter, and A. Zeilinger, Nature **390**, 575–579 (1997).
[4] N. Gisin, G. Ribordy, W. Tittel, and H. Zbinden, Rev. Mod. Phys. **74**, 145 (2002).
[5] L. Amico, R. Fazio, A. Osterloh, and V. Vedral, Rev. Mod. Phys. **80**, 517 (2008).
[6] Z.-Z. Li, W. Chen, M. Abbasi, K. W. Murch, and K. B. Whaley, Phys. Rev. Lett. **131**, 100202 (2023).
[7] J. Zhang, Y.-L. Zhou, Y. Zuo, H. Zhang, P.-X. Chen, H. Jing, and L.-M. Kuang, Advanced Quantum Technologies **n/a**, 2300350 (2024).
[8] L. Mandelstam, J. Phys.(USSR) **9**, 249 (1945).
[9] L. Mandelstam and I. Tamm, in *Selected papers* (Springer, 1991) pp. 115–123.
[10] S. Deffner and S. Campbell, Journal of Physics A: Mathematical and Theoretical **50**, 453001 (2017).
[11] P. Cieśliński, W. Kłobus, P. Kurzyński, T. Paterek, and W. Laskowski, New Journal of Physics **25**, 093040 (2023).
[12] P. A. Miller and S. Sarkar, Phys. Rev. E **60**, 1542 (1999).
[13] F. M. Izrailev, Physics Reports **196**, 299 (1990).
[14] M. Santhanam, S. Paul, and J. B. Kannan, Physics Reports **956**, 1 (2022).
[15] S. Paul, H. Pal, and M. S. Santhanam, Phys. Rev. E **93**, 060203 (2016).
[16] S. Paul and M. S. Santhanam, Phys. Rev. E **97**, 032217 (2018).
[17] F. L. Moore, J. C. Robinson, C. F. Bharucha, B. Sundaram, and M. G. Raizen, Phys. Rev. Lett. **75**, 4598 (1995).
[18] B. Gadway, J. Reeves, L. Krinner, and D. Schneble, Phys. Rev. Lett. **110**, 190401 (2013).
[19] S. Adachi, M. Toda, and K. Ikeda, Phys. Rev. Lett. **61**, 659 (1988).
[20] J. WANG and A. M. GARCIA-GARCIA, International Journal of Modern Physics B **22**, 5261 (2008), https://doi.org/10.1142/S0217979208049480.
[21] S. Sarkar, S. Paul, C. Vishwakarma, S. Kumar, G. Verma, M. Sainath, U. D. Rapol, and M. S. Santhanam, Phys. Rev. Lett. **118**, 174101 (2017).
[22] S. Paul, S. Sarkar, C. Vishwakarma, J. Mangaonkar, M. S. Santhanam, and U. Rapol, Phys. Rev. E **100**, 060201 (2019).
[23] S. Paul, J. B. Kannan, and M. S. Santhanam, Phys. Rev. E **108**, 044208 (2023).
[24] T. S. Monteiro, P. A. Dando, N. A. C. Hutchings, and M. R. Isherwood, Phys. Rev. Lett. **89**, 194102 (2002).
[25] B. V. Chirikov, F. M. Izrailev, and D. L. Shepelyansky, Sov. Sci. Rev. C **2**, 209 (1981).
[26] F. Izrailev and D. L. Shepelyanskii, Theoretical and Mathematical Physics **43**, 553 (1980).
[27] I. Talukdar, R. Shrestha, and G. S. Summy, Phys. Rev. Lett. **105**, 054103 (2010).
[28] L. Zhou and J. Gong, Phys. Rev. A **97**, 063603 (2018).
[29] N. Bolik, C. Groiseau, J. H. Clark, G. S. Summy, Y. Liu, and S. Wimberger, Phys. Rev. A **106**, 043318 (2022).
[30] B. Daszuta and M. F. Andersen, Phys. Rev. A **86**, 043604 (2012).
[31] E. Doron and S. Fishman, Phys. Rev. Lett. **60**, 867 (1988).
[32] S. Paul and A. Bäcker, Phys. Rev. E **102**, 050102 (2020).
[33] A. Lakshminarayan, Phys. Rev. E **64**, 036207 (2001).
[34] A. Lakshminarayan, S. C. L. Srivastava, R. Ketzmerick, A. Bäcker, and S. Tomsovic, Phys. Rev. E **94**, 010205 (2016).
[35] S. Tomsovic, A. Lakshminarayan, S. C. L. Srivastava, and A. Bäcker, Phys. Rev. E **98**, 032209 (2018).
[36] J. J. Pulikkottil, A. Lakshminarayan, S. C. L. Srivastava, M. F. I. Kieler, A. Bäcker, and S. Tomsovic, Phys. Rev. E **107**, 024124 (2023).
[37] J. J. Pulikkottil, A. Lakshminarayan, S. C. L. Srivastava, A. Bäcker, and S. Tomsovic, Phys. Rev. E **101**, 032212 (2020).
[38] A. Streltsov, G. Adesso, and M. B. Plenio, Rev. Mod. Phys. **89**, 041003 (2017).